

Published in final edited form as:

ACS Macro Lett. 2012 February 24; 2012(1): 384–387. doi:10.1021/mz200118f.

Hydrogen-bonded Multilayers of Silk Fibroin: From Coatings to Cell-mimicking Shaped Microcontainers

Veronika Kozlovskaya[†], Jennifer Baggett[†], Biana Godin[§], Xuewu Liu[§], and Eugenia Kharlampieva^{†,*}

[†]Department of Chemistry, University of Alabama at Birmingham, Birmingham, Alabama, 35294, USA

[§]Department of Nanomedicine, The Methodist Hospital Research Institute, Houston, Texas, 77030, USA

Abstract

We present a novel type of all-aqueous non-ionic layer-by-layer films of silk fibroin with synthetic macromolecules and a natural polyphenol. We found the multilayer growth and stability to be strongly pH-dependent. Silk assembled with poly(methacrylic) and tannic acids at pH=3.5 disintegrated at pH~5; while silk/poly(N-vinylcaprolactam) interactions were stable at low and high pH values but resulting in thinner films at high pH. The results suggest that the intermolecular interactions are primary driven by hydrogen bonding with a considerable contribution of hydrophobic forces. We also demonstrated that cubical, spherical and platelet capsules with silk-containing walls can be constructed using particulate sacrificial templates. This work sets a foundation for future explorations of natural and synthetic macromolecules assemblies as biomimetic materials with tunable properties.

Keywords

hydrogen-bonded; layer-by-layer; polyelectrolyte multilayers; silk fibroin; poly(vinylcaprolactam); shaped microcapsules

Hydrogen bonding is crucial for protein folding and has also been exploited in polyelectrolyte complexes (PECs) in solutions and on surfaces.^{1,2} Rubner and Zhang and co-workers pioneered H-bonded nanostructured films based on layer-by-layer (LbL) adsorption of uncharged polymers on surfaces from polymer solutions.³ Sukhishvili et al. included electrically neutral polycarboxylic acids to form pH-sensitive H-bonded multilayers.⁴ H-bonded capsules composed of an ultrathin multilayer shell and a hollow core for loading functional compounds can be also obtained.⁵ When assembled from aqueous media, H-bonded LbL structures offer the advantage of being environmentally friendly which is attractive for biomedical and bioengineering applications.^{2,6}

Hydrogen bonding was also found to be an essential intermolecular interaction defining the exceptional strength of silk fibers.⁷ Silk fibroin, extracted from silkworm cocoons, has risen considerable attention due to its biocompatibility, biodegradability, high mechanical strength, and morphologic flexibility.^{8,10} Silk has a unique block-copolymer structure of

Corresponding Authors: ekharlam@uab.edu.

Supporting Information. Experimental details on silk processing and structure as well as PVCL synthesis, fluorescent labeling, film and capsule preparation, synthesis of inorganic templates, ellipsometry, *in situ* ATR-FTIR. This material is available free of charge via the Internet at <http://pubs.acs.org>.

hydrophobic β -sheet blocks presented by (Ala-Gly)_n-repeats linked by hydrophilic less ordered regions containing Tyr, Val, and ionized acidic and basic amino acids (see SI).⁸ Despite the predominant hydrophobic nature, silk can be obtained in water-soluble amorphous form (silk I) which has a predominantly random coil conformation and can be processed into films, gels, fibers, microspheres, and scaffolds.^{8,9} Silk I is metastable and undergoes molecular rearrangement into water-insoluble β -sheet-rich crystalline form (Silk II) upon spinning, drying, exposure to alcohols, and environmental changes. Silk I-silk II transition was exploited to produce all-silk LbL assembled films.^{10, 11}

Silk interactions with synthetic and biological macromolecules have been mostly studied in solutions. Silk I was found to form H-bonded PECs with keratin,¹² chitosan,¹³ hyaluronic acid,¹⁴ poly(vinyl alcohol),⁸ and poly(acrylonitrile-co-methyl acrylate).¹⁵ Much less explored is assembly of silk with macromolecules on surfaces. Recently, silk was assembled with chitosan into LbL films via a combination of hydrogen-bonding and electrostatic interactions.¹⁶

In the current study we explored the capability of silk fibroin to assembly with synthetic macromolecules such as poly(methacrylic acid) (PMAA) and poly(N-vinylcaprolactam) (PVCL) as well as with a natural polyphenol, tannic acid (TA) at low and neutral pH values. Both ultrathin LbL coatings and hollow microcontainers of various shapes are studied. We believe that coupling silk with biocompatible macromolecules via hydrogen bonding holds a considerable promise for designing novel bio-mimetic materials with controlled properties and improved biological compatibility.

Assembly of silk-fibroin (M_w 416,000) with PMAA (M_w 100,000), TA (M_w 1,700), and PVCL (M_w 36,000) was first explored on flat surfaces at pH=3.5 (0.01M phosphate buffer). The chemical structures of the components are presented in Scheme 1. As monitored by *in situ* ATR-FTIR, silk fibroin was successfully assembled with all three components. All films showed linear growth with bilayer thickness of 11 ± 2 nm, 11 ± 2 nm, and 13 ± 2 nm for silk/PMAA, silk/TA, and silk/PVCL films, respectively, as measured with ellipsometry. In contrast, assembly of silk with poly(N-vinylpyrrolidone) (PVPON), a homologue of PVCL, which lacks two methylene groups in the ring, failed.

To investigate pH-stability, films constructed at pH=3.5 were exposed to elevated pH values and monitored with *in situ* ATR-FTIR (Fig. 1). We found that silk/PMAA and silk/TA films are completely erased at higher pH values. The critical dissolution pHs, when 90% of film thickness retained on surfaces, are 4.5 and 5 for silk/PMAA and silk/TA, respectively. In contrast, silk/PVCL films showed only 20% mass loss with both components partially released. Moreover, silk was successfully assembled with PVCL at pH=7.5 giving bilayer thickness of 4 ± 0.5 nm. The result that films assembled at pH=7.5 are thinner than those made at pH=3.5 explains decrease in film thickness when pH was changed from 3.5 to 7.5 (Fig. 1D). As expected, no silk/PMAA and silk/TA films were formed at pH=7.5, which correlates well with the stability of those films at low pH but their disintegration at elevated pH.

Since silk is a block copolymer polyampholite, the mechanism of intermolecular binding in silk-based multilayers is complex.^{8b,9} Silk functional moieties are presented by acidic, basic, polar- and non-polar groups capable of electrostatic, hydrogen-bonding, and hydrophobic interactions.²⁰ The acidic (Asp and Glu) and basic (His, Lys, and Arg) groups show pK_a values of around 5 and 10, respectively, while hydroxyl groups are presented by Ser, Tyr, and Thr.²⁰

Our results show that silk interaction with PMAA and TA are strongly pH-dependent and results in films which are stable at low pH but disintegrate at elevated pH value. The FTIR

spectrum of silk/PMAA film evidences that carboxyl groups of PMAA ($pK_a \sim 6.0$) are fully protonated at the deposition pH (Fig. 1A). Likewise, phenolic groups of TA ($pK_a \sim 5-8.5$) are not ionized at pH=3.5 (Fig. 1B). The protonated hydroxyl groups of PMAA and TA are available for hydrogen bonding with carbonyl groups of silk amide units. In fact, H-bonded PECs of silk with proton-donating hyaluronic acid,¹⁴ poly(vinyl alcohol)⁸ and chitosan¹³ have been observed previously. Hydrogen bonding between protonated carboxylic groups of polycarboxylic acids and amide bonds of globular proteins have been also reported.²¹ Ionization of the hydroxyl groups of PMAA and TA at elevated pH results in disruption of silk/PMAA and silk/TA associations at pH=4.5 and 5, respectively (Fig. 1D). The dissociation of silk/PMAA and silk/TA is additionally induced by ionization of silk carboxyl groups (Glu and Asp, $pK_a \sim 5$).²⁰

Silk-containing films studied here resemble properties of hydrogen-bonded LbL films of neutral polymers and poly(carboxylic acids) and TA. Those films were stable at low pH when the polyacids were protonated but dissolved at elevated pH due to polyacid ionization.⁴ The latter agrees well with hydrogen-bonded mechanism of silk/PMAA and silk/TA assembly, at which multilayer growth and stability is controlled by solution pH. Higher stability of silk/TA system as compared to silk/PMAA film can be explained by the gradual TA ionization with pK_a ranging from 5 to 8.5.²² The ability of TA to stabilize H-bonded multilayers of synthetic polyelectrolyte was found earlier.¹⁹

In contrast to pH-sensitive silk/PMAA and silk/TA systems, silk assembly with non-ionisable PVCL should be purely non-ionic and rely on the proton-donating silk capability. In this case, PVCL carbonyls most probably interact with proton-donating silk moieties such as amide and hydroxyl (including carboxyl and phenolic) groups via hydrogen bonding. Indeed, silk amide, hydroxyl and amine moieties were found to associate with carbonyl groups of methyl acrylate to form hydrogen-bonded PECs.¹⁵ However, much higher pH-stability of silk/PVCL assemblies as compared to other systems (Fig. 1D) points to the existence of other, most likely hydrophobic, interactions between silk and PVCL at high pH values. Indeed, despite ionization of silk carboxyl groups at pH >7.5, film lost only ~20% of their thickness (Fig. 1D).

Hydrophobic forces play an important role in intermolecular binding. For example, they always accompany hydrogen bonding and electrostatically-driven interactions in protein/polyelectrolyte systems, such as hydrogen bonding between protonated carboxylic groups of PMAA and a globular protein films.²¹ Considering silk hydrophobic nature, stabilization of intermolecular hydrogen bonding by hydrophobic forces should be very significant in silk-containing films. It is clearly observed in silk/PVCL systems, showing that silk interacts with PVCL rather than with more hydrophilic PVPON. Enhanced interchain binding due to the extra methyl groups in PVCL was found previously in PVCL/PMAA and PVCL/poly(L-aspartic acid) LbL systems.^{5a,19}

Importantly, we found that interlayer hydrogen bonding did not alter silk random coil conformation. The FTIR spectra for all LbL systems show that silk major peaks center at 1644 cm^{-1} which is characteristic of prevalent amorphous structure of silk I (Figure 1A,B,C).²⁰ The result is in contrast to the previously observed transformation of silk I to silk II upon silk “complexation” with macromolecules via intermolecular H-bonds.⁸ The silk I-silk II transition was also required to stabilize silk-on-silk or silk-chitosan LbL films achieved through alcohol treatment or drying.^{10,11,16} The FTIR spectrum of a (silk)₄ film shows two peaks centered at 1688 and 1623 cm^{-1} , which evidences crystalline β -sheet-rich silk II (Fig. S1, SI). Unlike those systems driven by hydrophobic interactions of dehydrated silk II, in our case the preserved silk I conformation affords for H-bonded interactions with the macromolecules in aqueous solutions.

Finally, the multilayers discussed above were deposited on particulate templates of various geometries to obtain silk-containing capsules with diverse shapes. Recently, the geometry of drug delivery carriers attracted significant attention as one of the main parameters determining biological functions and, therefore, targeted delivery such as control over vascular dynamics and cellular uptake.^{17,18} In our study, monodisperse spherical silica, cubical MnCO_3 , and silicon platelets (hemispheres) with dimensions of 4, 3, and 2 μm , respectively, were explored as sacrificial templates (Fig. 2a,d,g; see SI). First, (silk/PVCL)₅ LbL multilayers were fabricated on the cores at pH=7.5 using a well-established centrifugation method (see SI).⁵ For fluorescent visualization, PVCL tagged with Alexa Fluor 488 was synthesized ($M_w=30,000$ Da) and deposited in the last bilayer. Hollow capsules were then obtained by dissolving the templates in acidic solutions followed by dialysis in deionized water (see SI). CLSM in transmitted light mode evidences the complete dissolution of the cores (Fig S2, SI). We found that despite different surface morphology and shapes of the templates, spherical, cubical, and platelet-like capsules were successfully obtained (Fig. 2c,f,i). As observed with CLSM, silk/PVCL capsules maintained the initial geometry of the templates including those of a complex platelet shape. 3D CLSM images evidence flat facets with well-defined corners and edges for cubic and platelet capsules, respectively (Fig. 2b,e,h). An SEM image of platelet (silk/PVCL)₅ capsules illustrates grainy morphology of the shell surface (S3, SI). Capsules of (Silk/PMAA)₄, and (silk/TA)₄ were also fabricated (Fig. S4, SI).

Considering, that the dimensions and the shape of the platelet capsules resemble those of the red blood cells, these capsules hold considerable potential as cell-mimicking particles. Moreover, remarkable mechanical properties of silk integrated with the non-ionic all-aqueous, and thus biocompatible, hydrogen-bonding assembly opens new opportunities to engineer particles with bio-mimicking properties as novel carriers for therapeutic and contrast enhancing agents.

In summary, novel silk I-containing multilayer films have been fabricated based on hydrogen bonding with a contribution of hydrophobic forces. Silk/PMAA and silk/TA films are stable at pH=3.5 but disintegrate at higher pH, while silk/PVCL films show growth at both low and high pH values. Capsules of complex shapes have been also fabricated by using particulate sacrificial templates. Our study introduces new fundamental aspects of silk-based assembly and provides a new platform for designing silk-biomimetic materials with by-design properties.

Supplementary Material

Refer to Web version on PubMed Central for supplementary material.

Acknowledgments

The authors thank David Kaplan (Tufts University) for providing silk fibroin solution. This work was supported by Award #P30EB011319 from the National Institute of Biomedical Imaging and Bioengineering (E.K.). B.G. and X.L. acknowledge the support from NIH U54CA143837 (CTO, PS-OC) and NIH 1U54CA151668-01 (TCCN, CCNE).

References

1. Hirschberg JHKK, Brunsveld L, Ramzi A, Vekemans JAJM, Sijbesma RP, Meijer EW. *Nature*. 2000; 407:167. [PubMed: 11001050]
2. Kharlampieva E, Kozlovskaya V, Sukhishvili SA. *Adv Mater*. 2009; 21:3053.
3. (a) Stockton WB, Rubner MF. *Macromolecules*. 1997; 30:2717.(b) Wang L, Wang ZQ, Zhang X, Shen JC, Chi LF, Fucks H. *Macromol Rapid Commun*. 1997; 18:509.

4. (a) Sukhishvili SA, Granick SJ. *J Am Chem Soc.* 2000; 122:9550.(b) Kharlampieva E, Sukhishvili SA. *Polymer Reviews.* 2006; 46:377.
5. (a) Kharlampieva E, Kozlovskaya V, Tyutina J, Sukhishvili SA. *Macromolecules.* 2005; 38:10523. (b) Kozlovskaya, Higgins VW, Chen J, Kharlampieva E. *ChemComm.* 2011; 47:8352.
6. Lutkenhaus JL, McEnnis K, Hammond PT. *Macromolecules.* 2007; 40:8367.
7. Keten S, Buehler MJ. *Nano Lett.* 2008; 8:743. [PubMed: 18269263]
8. (a) Wang X, Yucel T, Lu Q, Hu X, Kaplan DL. *Biomaterials.* 2010; 31:1025. [PubMed: 19945157] (b) Vepari C, Kaplan DL. *Prog Poly Sci.* 2007; 32:991.
9. Basal G, Deveci SS, Yalcin D, Bayraktar O. *J Appl Polym Sci.* 2011; 121:1885.
10. Wang X, Kim HJ, Xu P, Matsumoto A, Kaplan D. *Langmuir.* 2005; 21:11335. [PubMed: 16285808]
11. Shechelina O, Drachuk I, Gupta MK, Lin J, Tsukruk VV. *Adv Mater.* 2011; 23:4655. [PubMed: 21915919]
12. Vasconcelos A, Freddi G, Cavaco-Paulo A. *Biomacromolecules.* 2008; 9:1299. [PubMed: 18355027]
13. Chen X, Li W, Zhong W, Lu Y, Yu T. *J Appl Polym Sci.* 1997; 65:2257.
14. Hu X, Lu Q, Sun L, Cebe P, Wang X, Zhang X, Kaplan DL. *Biomacromolecules.* 2010; 11:3178.
15. Sun Y, Shao Z, Hu P, Yu T. *J Polym Sci B: Polym Phys.* 1998; 35:1405.
16. Nogueira GM, Swiston AJ, Beppu MM, Rubner MF. *Langmuir.* 2010; 26:8953. [PubMed: 20158176]
17. Godin B, Tasciotti E, Liu X, Serda RE, Ferrari M. *Acc Chem Res.* 10.1021/ar200077p
18. Yoo J-W, Mitragotri S. *Proc Natl Acad Sci USA.* 2010; 107:11205. [PubMed: 20547873]
19. Erel-Unal I, Sukhishvili SA. *Macromolecules.* 2008; 41:8737.
20. (a) Matsumoto A, Chen J, Collette AL, Kim U-J, Altman GH, Cebe P, Kaplan DL. *J Phys Chem B.* 2006; 110:21630. [PubMed: 17064118] (b) Sashina ES, Bochek AM, Novoselov NP, Kirichenko DA. *Russ J Appl Chem.* 2006; 6:869.
21. Izumrudov V, Kharlampieva E, Sukhishvili SA. *Biomacromolecules.* 2005; 6:1782. [PubMed: 15877405]
22. Lin D, Liu N, Yang K, Zhu Z, Xu Y, Xing B. *Carbon.* 2009; 47:2875.
23. Shutava T, Prouty M, Kommireddy D, Lvov Y. *Macromolecules.* 2005; 38:2850.

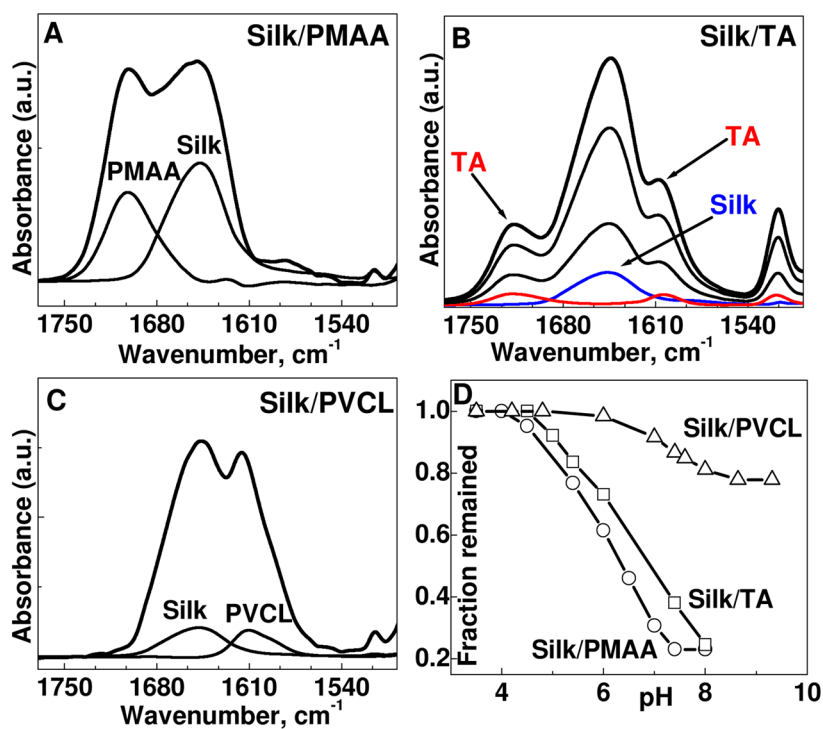


Figure 1. Sequential deposition of (silk/PMAA)_n (A), (silk/TA)_n (B), and (silk/PVCL)_n (C) from 0.5 mg/mL solutions at pH 3.5 as monitored by *in situ* ATR-FTIR. Silk random-coil conformation is presented by the vibrational peaks at 1644 cm^{-2} (A, B, and C). The absorption bands associated with protonated carboxylic groups ($-\text{COOH}$) are centered at 1700 cm^{-1} (A); carbonyl vibration band of the TA ester groups is located at 1716 cm^{-1} (B); and carbonyl of PVCL is centered at 1610 cm^{-2} (C). Evolution of total film disintegration as followed by *in situ* ATR-FTIR in the 1550–1800 cm^{-1} range (D).

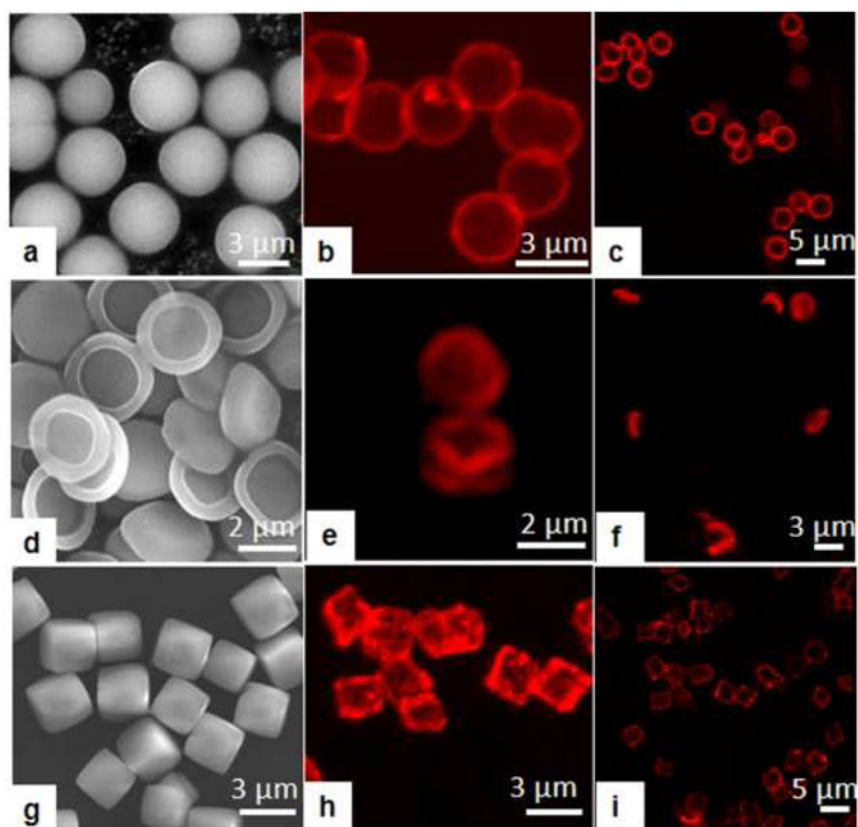
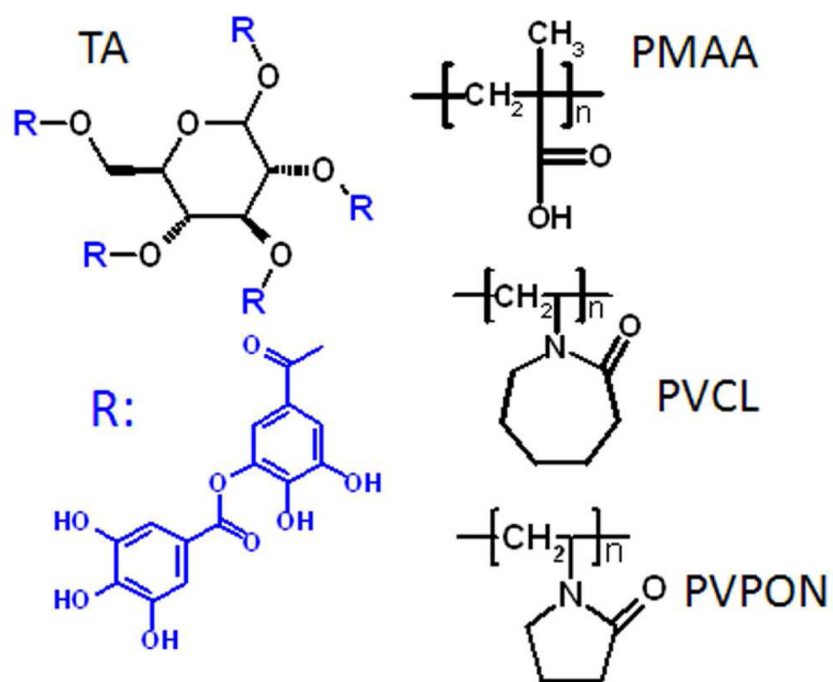


Figure 2. SEM images of spherical silica (a), hemispherical silicon platelets (d), cubical MnCO₃ (g); and CLSM images of (silk/PVCL)₅ capsules (b, c,e,f,h,i).



Scheme 1.
Chemical structures of TA, PMAA, PVCL, and PVPON used for assembly with silk fibroin.